

SPECTRAL REFLECTANCE SIGNATURES OF CASE II WATERS: POTENTIAL FOR TROPICAL ALGAL BLOOM MONITORING USING SATELLITE OCEAN COLOUR SENSORS

Soo Chin LIEW^{(a)♦}, I-I LIN^(a), Leong Keong KWOH^(a), Michael HOLMES^(b,c),
Serena TEO^(c), Karina GIN^(d) and Hock LIM^(a)

^(a)Centre for Remote Imaging, Sensing and Processing, ^(b)Department of Biological Sciences,
^(c)Tropical Marine Science Institute, and ^(d)Department of Civil Engineering
National University of Singapore, Kent Ridge, Singapore 119260

ABSTRACT

Sea-truth water sampling campaigns were carried out in the Johore Strait, Singapore from Dec 1996 to Dec 1998, partially funded by NASDA-ESCAP for utilization of ADEOS OCTS data. Water leaving radiance and reflectance data were collected together with coincidental measurements of water quality parameters, including the total suspended solid (TSS) and the chlorophyll-a (Chl-a) loadings. Results of spectral analysis show that, it is possible to distinguish case II waters of different TSS and Chl-a loadings as well as different phytoplankton bloom types using the reflectance spectra. Implications for remote sensing monitoring of algal blooms and retrieval of water quality parameters are discussed.

1. INTRODUCTION

Optical remote sensing is increasingly being used for monitoring of water quality parameters in the ocean, coastal waters as well as inland lakes and rivers¹⁻⁶. In optical remote sensing of water, the spectral reflectance, i.e. the ratio of the upwelling to downwelling irradiances at the water surface, is the radiometric quantity most often used in characterising the optical properties of water. There are three main classes of optically active constituents of sea water: coloured dissolved organic matter (CDOM), phytoplanktons and non-chlorophyllous particulate matter suspended in water^{1,3}. Of these constituents, the phytoplankton concentration and its spatial distribution is of particular interest not only to the marine scientists, but also to those involved in the fishery industry. Several algorithms exist for detecting phytoplankton pigments from ocean colour^{3,4,5}.

In the ocean, phytoplanktons (or algae) constitute the base of the marine food web. Phytoplankton concentration is correlated to the ocean primary production. The identification and monitoring of phytoplankton concentration are often considered as a viable means to locate new fishing grounds. However, certain types of algae blooms are not beneficial. The terms 'Harmful Algal Bloom (HAB)' or 'Red Tides' are often used to describe algal blooms which causes negative impacts to humans^{7,8}. Algal blooms may cause harm by shading other aquatic life. When bloom collapses, the microbial respiration on the dead and decaying cells can lead to reduced oxygen concentrations that can kill fish and other aquatic organisms due to lack of oxygen. In situation whereby a bloom is dominated by toxic algal species, toxins can be accumulated in the food chain and eventually be consumed by humans to cause paralytic or diarrhetic shellfish poisoning. HABs have caused severe damage to fishing industry and resulted in human casualties. In April 1998, Hong Kong fishery industries were

♦ Corresponding author: Dr. S. C. Liew, Centre for Remote Imaging, Sensing and Processing,
National University of Singapore, Blk. S17 Lower Kent Ridge Road, Singapore 119260.
Tel: (65) 8745069, Fax: (65) 7757717, Email: liew_soo_chin@nus.edu.sg

wiped off by a HAB episode which resulted in a loss of more than 10 million US dollars. In the summer of 1998, at least two persons were killed in the Philippines due to consumption of HAB polluted shellfish.

It is important to monitor occurrences of algal blooms due to their strong social, economic and health impacts. Traditional monitoring programmes by in situ point measurements are expensive, time consuming and inadequate since they do not have sufficient spatial and temporal coverage to monitor the complex dynamic phenomena occurring during a red tide episode. Satellite remote sensing measurement of ocean colour provides a feasible complementary tool for red tide monitoring, due to its synoptic coverage, frequent revisit capability and relatively low cost. As the individual phytoplankton pigments are characterised by their unique light absorbance features, detection of specific optical features can discriminate individual pigments. This property allows detection of algal blooms by ocean colour remote sensing technique.

Many factors contribute to the difficulty in monitoring algal blooms in coastal waters. Thousands of algal bloom species exist and algae blooms are usually transient phenomena. In addition, algae blooms co-exist with other constituents in the water body, majority of which are sediments and dissolved organic matter (yellow substance). The presence of these other constituents may obscure the optical signatures of algal blooms. Furthermore, due to the complexity of the problem, it is crucial to have large amount of *in situ* sea-truth data to help in the interpretation of remote sensing data.

In this work, spectral reflectance data acquired during a two-year sea-truth sampling programme in Singapore coastal waters are analysed. Attenuation coefficients of water in the visible and near-infrared region (from 400 to 750 nm) are derived from the reflectance spectra. It is possible to differentiate between coastal waters with different total suspended solid (TSS) and chlorophyll-a (Chl-a) loadings using the reflectance spectra. During the two-year campaign, spectral reflectance signatures of seven classes of algal blooms have been collected, including one class collected from the Manila Bay during the HAB episode in September 1997. The preliminary results in the classification of the reflectance spectra using the singular value decomposition (SVD) technique indicate that it is possible to discriminate the different classes of algal blooms from their respective reflectance spectra. The analysis of the spectra provides a basis for classification of the bloom types from satellite ocean colour and hyperspectral reflectance data.

2. DESCRIPTION OF DIFFERENT ALGAL BLOOM CLASSES

In this research, seven different classes of algal blooms were studied. These seven bloom classes were Trichodesmium (cyanobacteria), chain-forming diatom, mixed diatom and dinoflagellates (low), mixed diatom and dinoflagellates (high), Cochlodinium, small armoured dinoflagellate, and dinoflagellates from Manila Bay. Among the seven bloom classes, six bloom-samples were collected in Johor Strait, Singapore while one bloom was from Manila Bay, Philippines.

During the two-year sampling in Singapore, many of the bloom events were from diatoms, especially chain-forming diatoms. "Mixed diatom and dinoflagellate" blooms were blooms in which both diatom and dinoflagellate dominate. There were two such classes, one of higher dinoflagellate cell counts and the other of lower dinoflagellate cell counts. Both the cochlodinium and small armoured dinoflagellate blooms were dinoflagellate blooms. The major species in the Manila Bay dinoflagellate samples was *Ceratium furca*. There was also *Pyrodinium bahamense* (var. *compressum*) which was the notorious toxic red tide species that occurred in Manila Bay annually. Two reference sea water classes were used for comparison,

one from Johor Strait, Singapore and the other from the Manila Bay. These reference samples contained low phytoplankton counts.

3. METHODS

The sea-truth water sampling campaigns were carried out from Dec 1996 to Dec 1998. Reflectance spectra were acquired using a portable GER 1500 spectroradiometer. The water quality parameters measured were, among other things, the total suspended solid (TSS), chlorophyll-a (Chl-a), dissolved organic matter (DOM), total phosphate, total nitrogen and plankton cell count.

Attenuation coefficient of the sea water (for non-algal bloom case) was derived from each reflectance spectrum using an algorithm similar to the one reported by Sydor et. al.⁹ In this algorithm, the reflectance of water is modeled by the equation¹⁰,

$$R(\lambda) = A \frac{b(\lambda)}{a(\lambda) + b(\lambda)} \quad (1)$$

where $a(\lambda)$ is the absorption coefficient of the sea water and $b(\lambda)$ is the scattering coefficient. The sum $c(\lambda) = a(\lambda) + b(\lambda)$ is the attenuation coefficient of the sea water. The parameter A in this equation is only weakly dependent on wavelength and can be regarded as a constant. The scattering coefficient is modeled by the power law relation¹¹:

$$b(\lambda) = B \left(\frac{\lambda_{ref}}{\lambda} \right)^\alpha \quad (2)$$

where λ_{ref} is a reference wavelength, taken to be 550 nm, B and α are two parameters to be determined. In the long wavelength limit ($\lambda > 700$ nm), the attenuation coefficient is assumed to be due entirely to absorption by water. The product AB and the exponent α can then be determined by least square fitting of the observed reflectance spectra to the model relation (Equation 1). The attenuation coefficient for the whole visible wavelength range can then be evaluated using the same model.

An algorithm was tested for classification of the algal bloom types from the reflectance data. Suppose that $R_j(\lambda)$ is a reflectance spectrum measured for a given algal bloom class- j . For each algal bloom class- i , we seek a key vector $V_i(\lambda)$ such that the dot product of $R_j(\lambda)$ with $V_i(\lambda)$ is one if $j = i$, and zero if $j \neq i$. Using a training set of spectra of known classes, the key vectors for each class can be obtained using the singular value decomposition technique. After the key vectors have been determined, they are applied to each of the unknown spectra $R(\lambda)$ to be classified, by forming the dot-product:

$$w_i = \sum_{\lambda} R(\lambda) V_i(\lambda) \quad (3)$$

The dot product w_i is the score value of the reflectance spectrum with respect to class- i . If the unknown spectrum belongs to class- i , then the score value w_i assumes a value close to one, otherwise, the value is close to zero.

4. RESULTS

(a) Reflectance Spectra of Case II Sea Water

Typical reflectance spectra of the case II sea water samples around Singapore are shown in Figure 1 for four combinations of TSS and Chl-a loading: low TSS, low Chl-a; low TSS, high Chl-a; high TSS, low Chl-a and high TSS, high Chl-a. The reflectance spectra have been normalised such that they have the same mean reflectance value, in order to compensate for the possible scaling error in the measurements of the spectra.. For the clear sea water samples

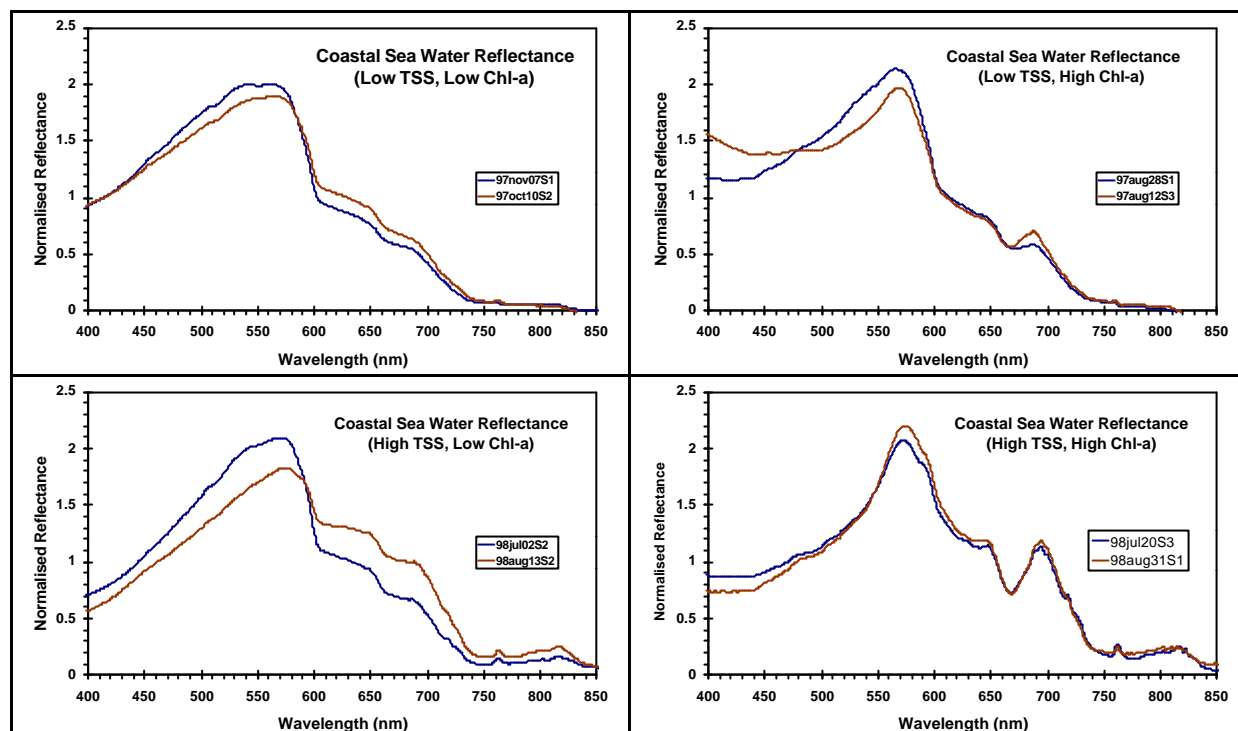


FIGURE 1: Representative reflectance spectra of coastal Case II sea water around Singapore. Top left: Low TSS (<10 mg/L) Low Chl-a (<3 $\mu\text{g/L}$); Top right: Low TSS High Chl-a (20 $\mu\text{g/L}$); Bottom left: High TSS (40-50 mg/L) Low Chl-a; Bottom right: High TSS (50 mg/L) High Chl-a (40 $\mu\text{g/L}$)

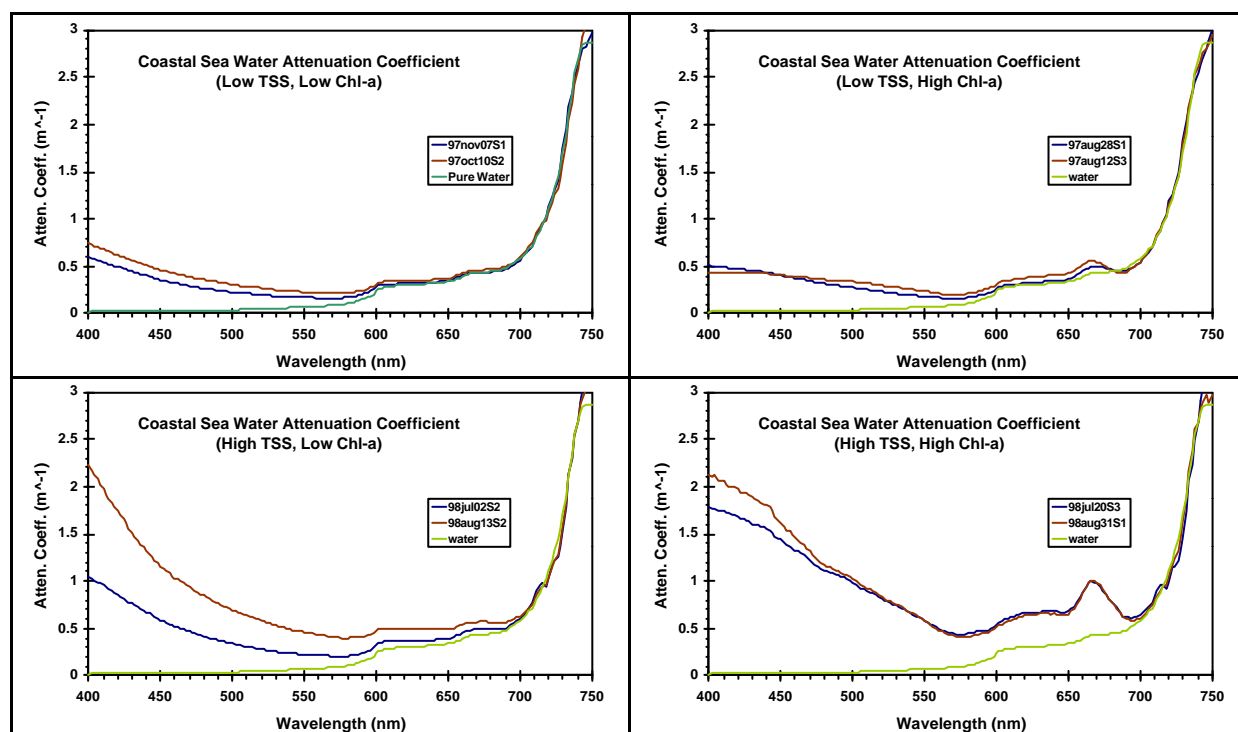


FIGURE 2: Attenuation coefficients of case II waters derived from the representative reflectance spectra shown in Figure 1. Top left: Low TSS (<10 mg/L) Low Chl-a (<3 $\mu\text{g/L}$); Top right: Low TSS High Chl-a (20 $\mu\text{g/L}$); Bottom left: High TSS (40-50 mg/L) Low Chl-a; Bottom right: High TSS (50 mg/L) High Chl-a (40 $\mu\text{g/L}$)

(top left panel of figure 1) of low TSS ($< 10 \text{ mg/l}$), low chlorophyll ($< 3 \text{ mg/m}^3$), and low phytoplankton counts ($< 100 \text{ cells/l}$). It can be seen from the figure that there is only 1 peak at 560nm in the green region which is typical for case-II waters. When the TSS loading is increased while Chl-a remains low (bottom left panel of figure 1), the shape of the reflectance spectra is about the same, but there seems to be an increase in the reflectance at longer wavelengths in the red and near-infrared regions. For Chl-a loaded water samples (top right and bottom right panels of Figure 1), the peak at 550 nm is narrower, and the absorption due to Chl-a at 667 nm results in a dip in the reflectance spectra.

Figure 2 shows the attenuation coefficients of case II water samples derived from the reflectance spectra shown in Figure 1. For low TSS samples, the attenuation coefficient curves are close to that of pure water for wavelength above 600 nm, and increases in the short wavelength (about 0.5 m^{-1} at 400 nm) due mainly to absorption by the dissolved organic matter present in the water. A peak at 667 nm for the low TSS but high Chl-a water sample can be observed, due to absorption by Chl-a. For high TSS samples, the attenuation at the short wavelength region increases further, due to the contribution from scattering by the suspended particulates. Influence from the particulate scattering component is evident up to wavelength of about 700 nm. The Chl-a absorption peak at 667 nm can clearly be seen.

The results show that the influence of the TSS and Chl-a components on the attenuation spectra of case II waters derived from the reflectance spectra can be distinguished.

(b) Reflectance spectra of phytoplankton blooms

From the collected spectral-radiometric spectra, it is found that different bloom classes are characterised by different spectra shapes. In this section, spectra from *Trichodesmium*, and chain forming diatom classes (shown in Figure 3) are discussed. The spectra shown in Figure 3 has been normalised equal mean and standard deviation. *Trichodesmium* is a species of cyanobacteria (blue-green algae). It is commonly found in the region of south east Asia and Australia. Although not a toxic phytoplankton species, it has been reported to cause death of fishes in Thailand, Indonesia, and Malaysia. The reflectance spectra of *Trichodesmium* bloom shown here were acquired during a bloom occurring on 30th-31st July 1997 at the eastern part of Singapore off Bedok coast. The bloom was characterised by orange-brown patches with typical dimension 0.5m by 5m. The *Trichodesmium* count was estimated to be 210,000 cells/l. Figure 3 (left panel) illustrates typical spectra of *Trichodesmium*. The chlorophyll absorption bands at 443 nm and 660 nm can be clearly seen. Another clear trough is found around 490nm corresponding to the pigment absorption.

Chain forming diatom blooms are the most common type of phytoplankton bloom which occurred in the Johor Strait, Singapore. In general, most tropical diatoms belong to non-toxic species. Figure 3 (right panel) shows typical spectra of such blooms. It can be seen from the figure that the spectral characteristics of chain forming diatom bloom is very different from *Trichodesmium* and clear water spectra (top left panel of Figure 1). Besides the 560nm peak of case 2 sea water, there is another peak found at around 690nm region. The absorption at 670 nm is clearly visible, but unlike the *Trichodesmium* spectra, there are no distinct peaks and troughs in other bands.

(c) Spectral analysis of algal bloom reflectance spectra

Results of spectral analysis for algal bloom types classification using various combinations of reflectance difference and reflectance ratio at several wavelength bands have been reported previously¹². Use of different band combinations results in discrimination of

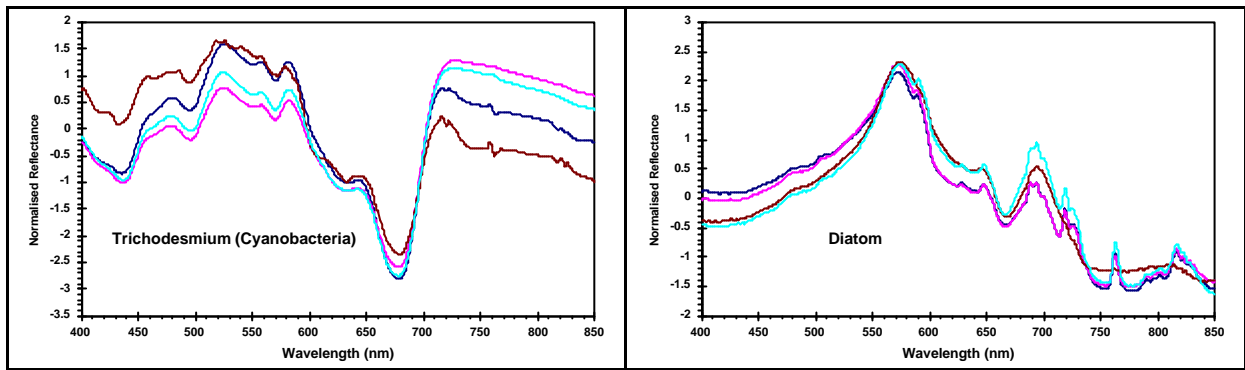


FIGURE 3: Representative reflectance spectra of algae blooms observed in Singapore waters. Left: Trichodesmium (cyanobacteria); Right: Chain forming diatoms.

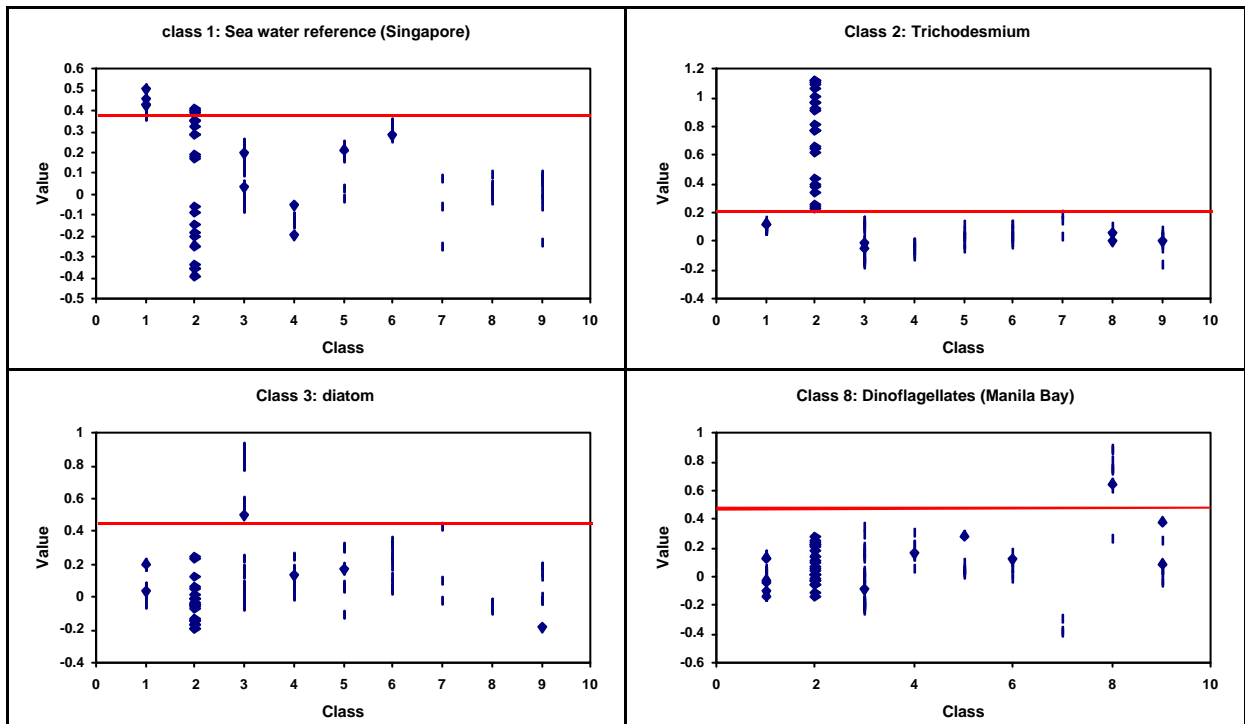


FIGURE 4: Results of spectral analysis of the algal bloom spectra using the SVD technique. See text for details. The nine classes are: 1. Reference sea water (Singapore), 2: Trichodesmium, 3: Diatoms, 4: Mixed diatom and dianoflagellate (high dinoflagellate count), 5: Mixed diatom and dianoflagellate (low dinoflagellate count), 6: Cochloclinium (Dianoflagellate), 7: Armoured Dianoflagellate, 8: Ceratium and Pyrodinium Bahamense (Manila Bay samples), 9: Reference sea water (Manila Bay).

different algal bloom types. Among the nine classes (seven algal bloom classes, two clear water classes), seven classes could be unambiguously separated.

In this paper, the preliminary results of using singular value decomposition technique in classification of the reflectance spectra are reported. This technique makes use of the information contains in all the available wavelength channels, instead of selecting a small subset of the channels for analysis. Some representative results of classification using this technique is illustrated in Figure 4. In each panel of Figure 4, the score values w_i (evaluated using Equation 3) of all the reflectance spectra for all the nine algal bloom classes with respect to a given class- i are plotted.

For example, in the top left panel of Figure 4, the score values of all spectra are evaluated with respect to the key vector for Singapore reference sea water (class-1). By using a threshold value of 0.39, almost all samples from the reference sea water class are correctly

classified, while all other spectra except two from class-2 (*Trichodesmium*) are correctly classified as not belonging to class-1. The top right panel of Figure 4 shows that all samples are correctly classified with respect to class-2 (*Trichodesmium*) if a threshold of 0.2 is used. In the bottom left panel, 31 out of a total of 40 spectra from class-3 (Diatom) can be correctly separated from the rest. The 9 misclassified spectra were all acquired on the same date, from the same site. On re-examination of the spectra, the shapes of these spectra were found to be visually different from the other spectra. The bottom right panel shows that all except one of the spectra from class-8 (*Ceratium* and *Pyrodinium Bahamense* from Manila Bay) are correctly classified. Two other classes (class-7 and class-9, results not shown) are also correctly classified. In summary, six out of the nine classes can be discriminated with a reasonably good accuracy. The other three classes show a greater degree of confusion.

5. DISCUSSIONS AND CONCLUSIONS

This research studied the spectral characteristics of case II sea water. The reflectance spectra were collected during a two-year sea-water sampling programme in coastal waters around Singapore. The attenuation coefficients of the sea water samples were derived from the reflectance spectra. Coastal waters with different TSS and Chl-a loadings could be distinguished from the attenuation spectra. The results indicate that it is possible to retrieve the water quality parameters from the reflectance spectra acquired above the water surface.

Seven types of algal blooms have also been observed and studied during the two-year campaign. Six of them were observed in Singapore water, while the other one was observed during a field trip to the Manila Bay in September 1997. These algal bloom classes are characterised by different spectral signatures. The peaks and troughs observed in the spectra are related to different phytoplankton properties, e.g., chlorophyll-a absorption, and pigment absorption. A classification algorithm based on the singular value decomposition technique has been tested on the reflectance spectra. Six out of nine classes (including two reference sea water classes) can be discriminated with good accuracy. The result suggests the feasibility of differentiating algal bloom types by their reflectance spectra.

The spectral data used in this study were collected using a hand-held spectroradiometer, which measures light radiance in 512 wavelength bands continuously from 350 nm to 1050 nm. Currently, there is no satellite-borne sensors capable of acquiring this type of hyperspectral data. However, satellites with hyperspectral sensors will be launched in the near future (e.g. the Hyperion sensor on the planned NASA's EO-1 mission). The techniques developed here can be applied to the hyperspectral data acquired by satellite-borne sensors. Currently, the SeaWiFS sensor on board the SeaStar satellite (launched October 1997) is the only available satellite-borne ocean colour sensor. It has six bands in the visible region and two in the near-infrared region. Each band has 20 nm bandwidth. The other recent sensor was the OCTS onboard the Japan's ADEOS satellite launched in August 1996. ADEOS ceased operation in June 1997 when the ADEOS satellite stops its operation. It was the first second generation ocean color sensor after the 10 years gap since NASA's CZCS. Future planned ocean colour sensors include the NASA's MODIS, NASDA's ADEOS2-GLI and ESA's ENVISAT-MERIS. These future sensors have more wavelength bands with narrower bandwidths. Studies are currently being done in our group to evaluate these ocean colour sensors for their capabilities in retrieval of water quality parameters in coastal waters and algal bloom type classification, using data simulated from the in-situ hyperspectral reflectance data. Our preliminary results indicate that the GLI sensor is probably the best for these purposes. Further research is in progress to develop various techniques in utilising the spectral information for retrieval of water quality parameters and classification of algal bloom types.

6. ACKNOWLEDGEMENTS

This study was partially supported by the National Space Development Agency of Japan (NASDA) through the joint NASDA-ESCAP project entitled "National capacity building for sustainable environment and natural resources management through research and studies on the uses of ADEOS data". The authors wish to thank Prof. Rhodora Azanza of the Marine Science Institute, University of Philippines, for her assistance during the field trip to Manila Bay.

7. REFERENCES

1. S. Sathyendranath, L. Prieur, and A. Morel, A three component model of ocean color and its application to remote sensing of phytoplankton pigments in coastal waters. *Int. J. Remote Sens.* 10, 1373-1394, 1989.
2. H. R. Gordon and M. Wang. Retrieval of water-leaving radiance and aerosol optical thickness over the oceans with SeaWiFS: a preliminary algorithm, *Appl. Opt.* 33, 443-452, 1994.
3. R. Doerffer and J. Fischer, Concentrations of chlorophyll, suspended matter, and gelbstoff in case II waters derived from satellite coastal zone color scanner data with inverse modeling methods, *J. Geophys. Res.* 99, 7457-7466, 1994.
4. S. Sathyendranath, F. E. Hoge, T. Platt, and R. N. Swift, Detection of phytoplankton pigments from ocean color: improved algorithms, *Appl. Opt.* 33, 1081-1089, 1994.
5. S. Tassan, Local algorithms using SeaWiFS data for the retrieval of phytoplankton, igments, suspended sediment, and yellow substance in coastal waters, *Appl. Opt.* 33, 2369-2378, 1994.
6. R. W. Gould and R. A. Arnone, Remote sensing estimates of inherent optical properties in a coastal environment. *Rem. Sens. Environ.* 61, 290-301, 1998.
7. R. A. Corrales, and E.D. Gomez, *in Toxic Marine Phytoplankton*, pp.453-458, Elsevier, 1990.
8. K. Richardson, K. Harmful or Exceptional Phytoplankton Blooms in the Marine ecosystem. *Adv. Mar. Biol.* 31, 301-385, 1997.
9. M. Sydor, R. A. Arnone, R. W. Gould, Jr., G. E. Terrie, S. D. Ladner, and C. G. Wood. Remote sensing technique for determination of the volume absorption coefficient of turbid water, *Appl. Opt.* 37, 4944-4950, 1998.
10. S. Sathyendranath and T. Platt. Analytic model of ocean color, *Appl. Opt.* 36, 2620-2629, 1997.
11. C. D. Mobley, *Light and water*, Academic, 1994.
12. I-I Lin, V. Khoo, M. Holmes, S. Teo, S. T. Koh, and K. Gin, Tropical algal bloom monitoring by sea truth, spectral and simulated satellite data. *Proc. 1999 Int. Geosci. Rem. Sens. Symp.* Vol. 2, 931-933, 1999.